diversity

Article

Predicting the Potential Suitable Area of the Invasive Ant *Linepithema humile* in China under Future Climatic Scenarios Based on Optimized MaxEnt

Ming Li [1,†], Xiaoqing Xian [1,†], Haoxiang Zhao [1], Lin Xue [2], Baoxiong Chen [2], Hongkun Huang [2], Fanghao Wan [1] and Wanxue Liu [1,*]

[1] State Key Laboratory for Biology of Plant Diseases and Insect Pests, Institute of Plant Protection, Chinese Academy of Agricultural Science, Beijing 100193, China
[2] Rural Energy and Environment Agency, Ministry of Agriculture and Rural Affairs, Beijing 100125, China
* Correspondence: liuwanxue@caas.cn
† These authors contributed equally to this work.

Abstract: *Linepithema humile* (Mayr, 1868) (Hymenoptera: Formicidae) is one of "100 of the world's worst invasive alien species" listed by the International Union for Conservation of Nature and Natural Resources (IUCN). Although native to South America, this ant has spread worldwide via international trade. Currently, *L. humile* has not been found in China, and if it invades China, it might pose a potential risk to the native invertebrates, vertebrates, plants, and human livelihoods. Based on 2432 global occurrence records and ten bioclimatic variables, the optimized MaxEnt model was used to predict the potential suitable areas of *L. humile* in China. We analyzed the important bioclimatic variables affecting the potential suitable areas, and determined the changes in potential suitable areas under future climatic scenarios. Our results indicated that the mean temperature of the coldest quarter (Bio11), precipitation of the coldest quarter (Bio19), mean temperature of the wettest quarter (Bio8), and precipitation of the warmest quarter (Bio18) were the most important bioclimatic variables. Under the current climatic scenarios, the potential suitable area of *L. humile* in China is 80.31×10^4 km^2, which is mainly located in Fujian, Zhejiang, Hunan, Jiangxi, Guangxi, Yunnan, and Hubei. Under future climate scenarios over coming decades, the potential suitable areas of *L. humile* showed an overall increase and a shift to higher latitudes, which indicated the invasion risk of *L. humile* in China will increase under climate change. Our findings provide the theoretical guidance for the early warning and monitoring of *L. humile* in China.

Keywords: invasive alien ant; species distribution model; bioclimatic variable; overfitting; climate scenario

Citation: Li, M.; Xian, X.; Zhao, H.; Xue, L.; Chen, B.; Huang, H.; Wan, F.; Liu, W. Predicting the Potential Suitable Area of the Invasive Ant *Linepithema humile* in China under Future Climatic Scenarios Based on Optimized MaxEnt. *Diversity* **2022**, *14*, 921. https://doi.org/10.3390/d14110921

Academic Editor: Alan N. Andersen

Received: 8 September 2022
Accepted: 26 October 2022
Published: 28 October 2022

1. Introduction

Biological invasion is the process whereby non-native species are introduced into new areas in which they survive, reproduce, establish, and potentially expand their range [1]. Global trade has been the main driver of biological invasion [2], and with the rapid development of international trade over recent decades, the numbers of invasive alien species (IAS) and the detrimental impacts of invasion have been on the rise [3]. Biological invasions have a considerable effect on the biodiversity, ecological environment, and agricultural production of countries worldwide, and have accordingly become established as one of the five major global environmental issues of the 21st century [4]. Estimates based on recent global studies have put economic losses caused by IAS at up to $1.4 trillion per year, accounting for more than 5% of the global gross domestic product [5]. Therefore, biological invasion control should become one of the main concerns and work centers of all countries.

Ecologically, ants are among the most important insect species. Their small size and multifaceted nesting habits are conducive to human-mediated translocation [6], and as a consequence of the increasing growth in global trade, transportation, and tourism in recent decades, ants have accordingly been anthropogenically distributed beyond their native ranges. Five invasive alien ants (*Linepithema humile*, *Solenopsis invicta*, *Anoplolepis gracilipes*, *Wasmannia auropunctata*, and *Pheidole megacephala*) were listed among "100 of the world's worst invasive alien species" [7].

Linepithema humile is native to South America (Argentina, Uruguay, Brazil, and Paraguay), and has been introduced to six continents and several oceanic islands [8]. Currently, there are no occurrence records of *L. humile* in most of East Asia, including China. The social structure of *L. humile* is polygamous, and many workers and queens form large, high-density nests, thus promoting the spread to new areas of the species [9]. These factors have accordingly contributed to the success of *L. humile* as a strong competitor and invader [9]. *Linepithema humile* is a well-known agricultural and urban pest that can spread rapidly throughout suitable areas, reducing species richness, affecting the growth and development of plants, and causing economic losses in invaded areas. For example, *L. humile* has been found to compete with native ants in San Luis Obispo, California, causing significant declines in the populations of 10 native ant species [10]. Similarly, *L, humile* has been observed to reduce the numbers of arthropods (the main pollinators of inflorescences) in the Western Cape of South Africa by 32% to 62%, thereby severely affecting plant reproduction and growth [11,12]. Moreover, in New Zealand, the cost of controlling *L. humile* has reached millions of dollars [13]. Although to date there have been no reports of *L. humile* populations in China, this invasive ant has biological characteristics similar to those of *S. invicta*. Accordingly, to prevent any future introduction and establishment of *L. humile*, which poses a threat to biodiversity, agricultural production, and human health.

According to the Sixth Assessment Report of the Intergovernmental Panel on Climate Change (IPCC), global warming will rise by 1.5 °C or more in the coming two decades [14]. Insects are poikilothermic temperature animals, which was particularly sensitive to temperature variables [15]. Rapid climate warming affected the growth and development, egg laying, overwintering, distribution patterns, and reproductive rates of insects [16]. Previous studies have shown that global climate warming will affect the distribution of many species worldwide, including invasive alien ants, causing changes in distribution patterns and promoting migration to higher latitudes [17]. For instance, the potential suitable areas of *S. invicta* will increase and move to higher latitudes in China under climate change [18]. Consequently, paying more attention to the response of *L. humile* to climate change is helpful not only in understanding the changes in the distribution pattern but also in formulating early warning and management strategies to prevent the invasion of *L. humile* in China.

Species distribution models (SDMs) are numerical tools that integrate environmental data with data of a species' occurrence or abundance, and can predict the current and future potential suitable areas of the species [19–21]. The MaxEnt model has become the most commonly applied species distribution model, because of its small sample size requirement, simple operation, stable computing results, and short computing time [22–24]. Moreover, it performs well in predicting the regionally suitable distribution of IAS [25,26]. For instance, MaxEnt models were used to study the potential suitable area of the invasive ants *S. invicta* in China [27], and *A. gracilipes* in China and the world [28]. Using the default parameters to build a MaxEnt model is prone to overfitting, and results in less accurate model predictions [29,30]. Therefore, the ENMeval data package in the R software is used to optimize the parameters of the MaxEnt model to avoid model overfitting and improve the rationality and accuracy of species predictions [31].

In this study, we used the optimized MaxEnt model to predict the invasion risk of *L. humile* in China under current and future climatic scenarios. The main objectives of this study were: (1) to determine the important bioclimatic variables affecting the potential suitable area of *L. humile* in China, (2) to assess potential suitable areas of *L. humile* in China under current climatic scenarios, and (3) to determine changes in the potential suitable areas of *L. humile* in China under future climatic scenarios, and centroid shifts of potential suitable areas between current and future climatic scenarios. Our results would provide a scientific basis for continued monitoring and early warning of *L. humile* in China.

2. Materials and Methods

2.1. Global Occurrence Records of *Linepithema humile*

First, 10,371 global occurrence records of *L. humile* worldwide were obtained from the Global Biodiversity Information Facility (GBIF, https://www.gbif.org/, accessed on 27 June 2022) and the Invasive Species Compendium of the Center for Agriculture and Bioscience International (CABI, https://www.cabi.org/, accessed on 28 June 2022). Only one occurrence record was kept for each 5 × 5 km raster interval to prevent overfitting of the model using the ENMtools software for the species occurrence records. Once filtering was complete, 2432 occurrence records were retained for model construction (Figure 1).

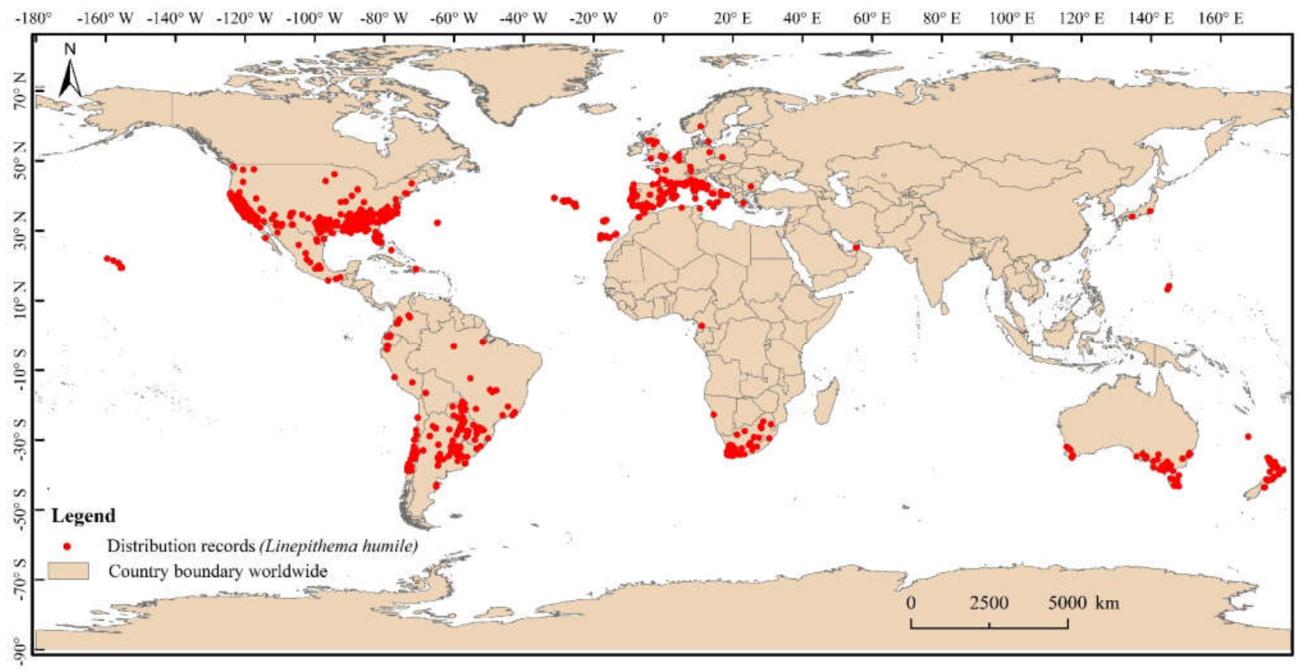

Figure 1. Global occurrence records of the *Linepithema humile.*

2.2. Bioclimatic Variables

A total of 19 bioclimatic variables were downloaded from the World Climate Database (http://www.worldclim.org/ accessed on 27 June 2022) at a resolution of 2.5′ under current and future climatic scenarios (Table 1). The bioclimatic climate variables under future climate scenarios included three shared socioeconomic pathways (SSP1-2.6, SSP2-4.5 and SSP5-8.5) for two periods (the 2030s and 2050s) under the BCC-CSM2-MR developed by the global climate model of the National Climate Center (Table S1).

Table 1. Bioclimatic variables are related to the distribution of *Linepithema humile.*

Variable	Description	Unit	Whether to Use for Modeling
Bio1	Annual mean temperature	°C	No
Bio2	Mean diurnal air temperature area	°C	Yes
Bio3	Isothermality (bio2/bio7) (*100)	—	No
Bio4	Temperature seasonality (standard deviation *100)	—	No

Bio5	Max temperature of warmest month	°C	Yes
Bio6	Min temperature of coldest month	°C	No
Bio7	Temperature annual area (bio5-bio6)	°C	Yes
Bio8	Mean temperature of wettest quarter	°C	Yes
Bio9	Mean temperature of driest quarter	°C	No
Bio10	Mean temperature of warmest quarter	°C	No
Bio11	Mean temperature of coldest quarter	°C	Yes
Bio12	Annual precipitation	mm	No
Bio13	Precipitation of wettest month	mm	No
Bio14	Precipitation of driest month	mm	No
Bio15	Precipitation seasonality (coefficient of variation)	—	Yes
Bio16	Precipitation of wettest quarter	mm	Yes
Bio17	Precipitation of driest quarter	mm	Yes
Bio18	Precipitation of warmest quarter	mm	Yes
Bio19	Precipitation of coldest quarter	mm	Yes

In order to avoid the result of the MaxEnt model overfitting due to the multicollinearity between the 19 bioclimatic variables. First, 19 bioclimatic variables were correlated in the spatial analyst tool in ArcGIS software; then the 19 bioclimatic variables and species occurrence records were imported into the MaxEnt model for 10 repetitions. If the two bioclimatic variables had a correlation coefficient with absolute values greater than 0.8 ($|r| > 0.8$), the bioclimatic variable with the higher contribution was retained (Figure S1) [32]. Finally, ten bioclimatic variables were used to construct the MaxEnt model (Table 1).

2.3. Optimized MaxEnt Modeling

The results of the MaxEnt model are prone to overfitting when modeling using the program's default settings. Feature combinations (FCs) and regularization multiplier (RM) are the two most important parameters in MaxEnt models [33]. FCs included linear-L, quadratic-Q, hinge-H, product-P and threshold-T. The RM was set 0.5 to 4, at intervals of 0.5. In this study, we used the ENMeval package in R software to adjust the parameters of FCs and RM choose to use the delta AICc minimum parameter combination as the optimal parameter setting for the model [34]. FCs and RM were set to LQHPT and 0.5, respectively.

2.4. Model Evaluation and Potential Suitable Area Delineation

The FC and RM were set up according to the optimal model, and 75% of the occurrence records were selected for simulation training and 25% for model testing. In the MaxEnt model, the maximum number of iterations was set to 500, the background points to 10,000, and the output format to Cloglog, and cross-validated by running 10 replicates. The jackknife method was chosen to test and create response curves to assess the effects of bioclimatic variables on the potential suitable area of *L. humile* in China. The accuracy of the model was examined using the area enclosed by the area of under receiver operating characteristic (ROC) curve (AUC) [35]. The model prediction accuracy evaluation is classified as excellent for 0.8–1, usable for 0.5–0.8, and poor for 0–0.5 [36].

The maximum value of 10 repetitions in the MaxEnt model was selected as the result of this study, and the potential suitable area of *L. humile* in China was cropped according to map of the country. The results were generated based on the presence probability of *L. humile*, with values in the range of 0–1, with larger values indicating higher species presence probability. We used the reclassify tool in ArcGIS software to classify the suitable habitat into four levels, 'highly suitable area' (0.5~1), 'moderately suitable area' (0.3–0.5), 'poorly suitable area' (0.1–0.3) and 'unsuitable area (0–0.1)'.

The spatial distribution of geographical objects can be described by the centroid, and the displacement of geographical objects over a period of time can be expressed using the centroid [37]. In this study, the regularity of potential habitat area displacement of *L. humile* was reflected by the change in the period of the potential habitat area. First, the habitat raster map was transformed into a vector map using the ArcGIS software. Then, the centroid of the potential habitat area was then calculated using the Statistical Analysis Zonal [37].

3. Results

3.1. Model Optimization and Accuracy Evaluation

Our results showed that delat.AICc is lowest when FCs are LQHPT and RM is 0.5, when Mean AUC is greater than the value at default parameters (Figure 2). Under the optimal parameter settings, the mean AUC value of the ten simulations based on the MaxEnt model for the current potential habitat area of *L. humile* was 0.883, indicating excellent model prediction accuracy and high stability (Figure 3).

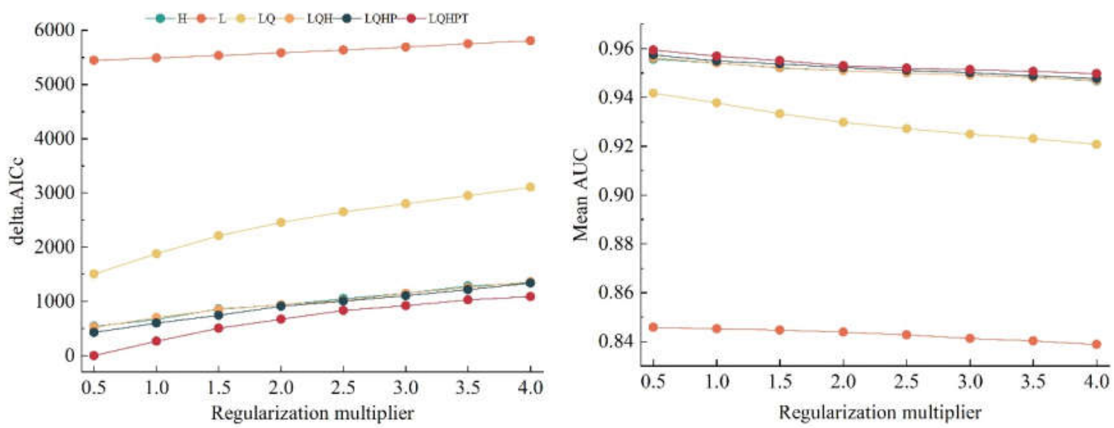

Figure 2. Optimal parameter results for the MaxEnt model.

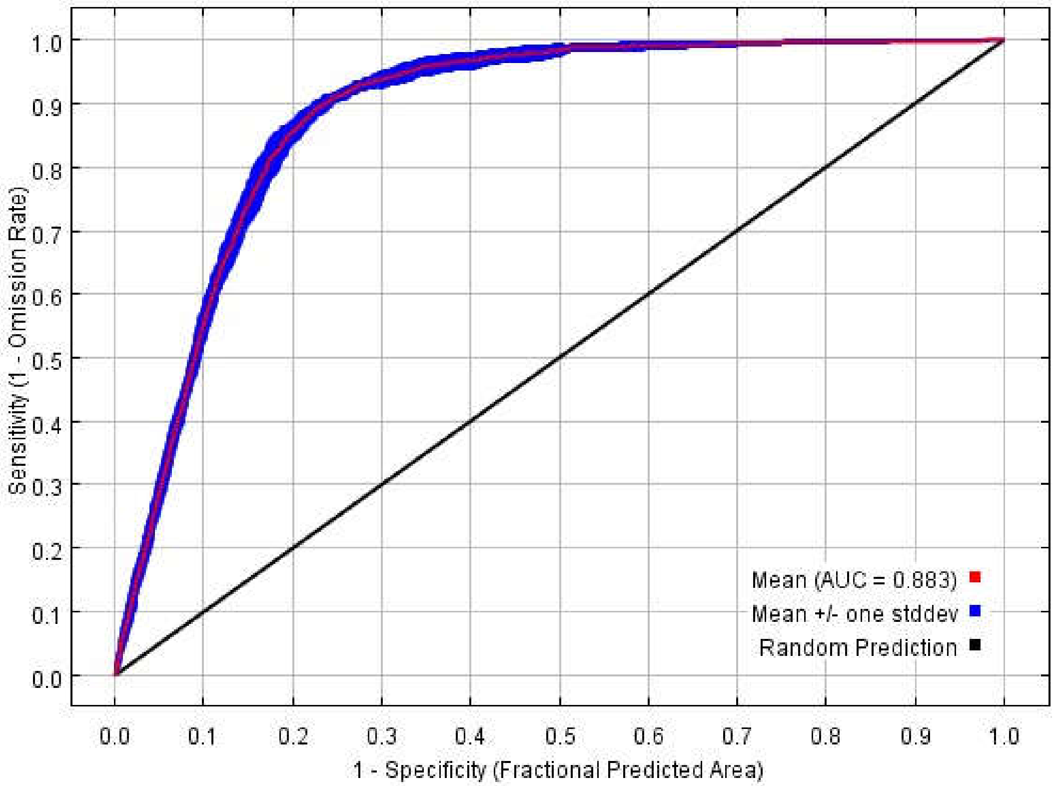

Figure 3. Mean AUC values of the *Linepithema humile* MaxEnt model.

3.2. Bioclimatic Variables Affecting the Potential Suitable Area of Linepithema humile

The mean temperature of the coldest quarter (Bio11), precipitation of the coldest quarter (Bio19), mean temperature of the wettest quarter (Bio8), and precipitation of the warmest quarter (Bio18) were the most important bioclimatic variables based on jackknife and percent contribution (Figures 4 and S2). The important bioclimatic variables affecting the potential suitable area of *L. humile* are two temperature (mean temperature of the coldest quarter, mean temperature of the wettest quarter) and two precipitation variables (precipitation of the coldest quarter, precipitation of the warmest quarter).

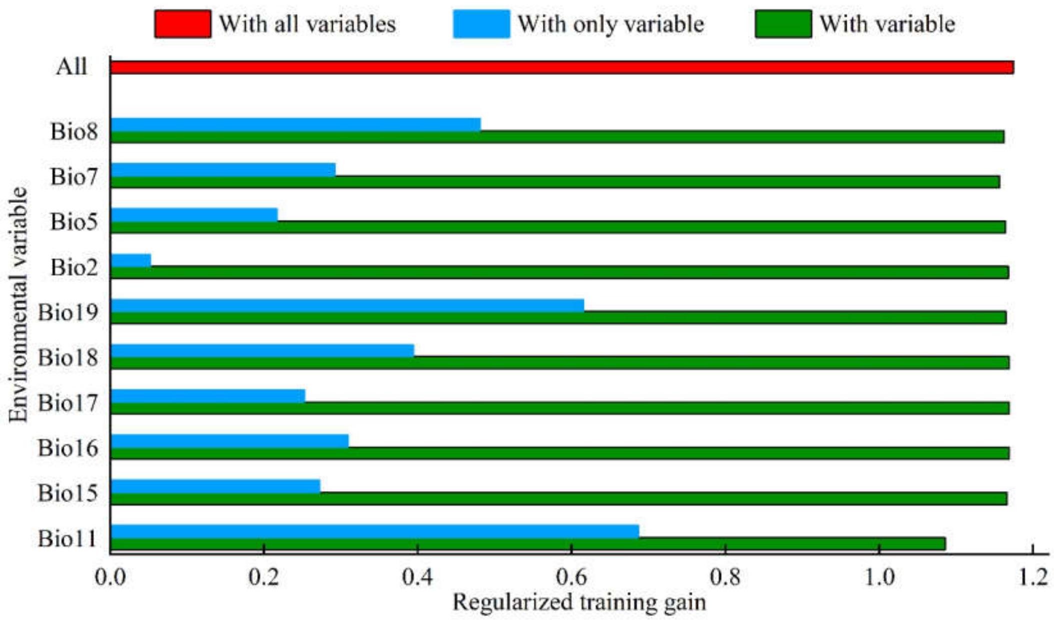

Figure 4. Jackknife test results for *Linepithema humile* bioclimatic variables.

The relationship between the probability of presence of *L. humile* and bioclimatic variables showed in Figure 5. When the probability of presence values of *L. humile* was greater than 0.5, it indicated that the corresponding interval of bioclimatic variables was suitable for the species. For temperature variables, the mean temperature of the coldest quarter (Bio11) and mean temperature of the wettest quarter (Bio8) ranged from 6.83 °C to 19.28 °C, and from 6.97 °C to 28.36 °C, respectively. For precipitation variables, the precipitation of the coldest quarter (Bio19) and precipitation of the warmest quarter (Bio18) ranged from 98.89 mm to 882.65 mm, and from 1.51 mm to 373.27 mm, respectively.

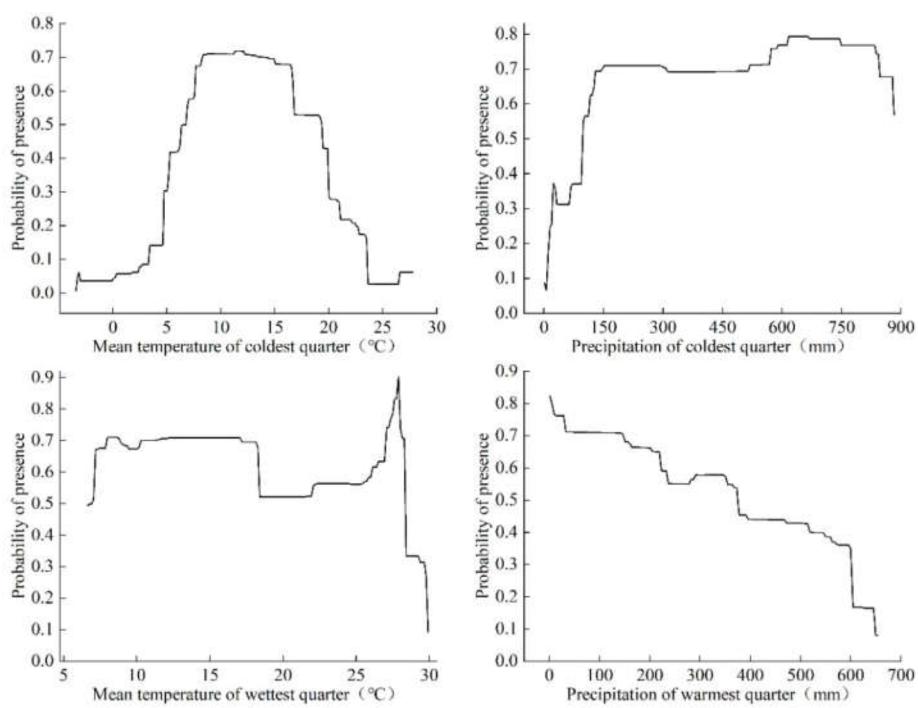

Figure 5. Probability of presence for important bioclimatic variables for *Linepithema humile*.

3.3. Current Potential Suitable Areas of Linepithema humile in China

The prediction of the potential suitable areas of *L. humile* in China under the current climate is shown in Figure 6. The total suitable area was 80.31 × 10^4 km^2 (Table S2), accounting for 8.36% of the total area of Chinese mainland, which was mainly located in southeast and southwest of China. The highly suitable area was 0.18 × 10^4 km^2, accounting for 0.02% of the total area of the Chinese mainland, which was mainly located in Fujian. The moderately suitable area was 6.37 × 10^4 km^2, accounting for 0.66% of the total area of the Chinese mainland, which was mainly located in Zhejiang, Fujian, Hunan, and Guangxi. The poorly suitable area was 73.76 × 10^4 km^2, accounting for 7.68% of the total area of the Chinese mainland, which was mainly located in Zhejiang, Fujian, Jiangxi, Hunan, Yunnan, and Hubei.

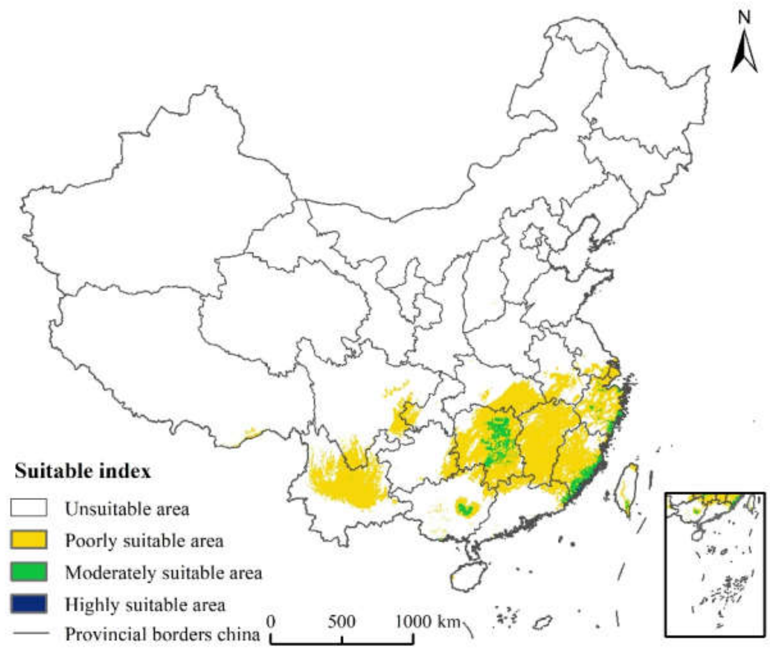

Figure 6. Potential suitable area for *Linepithema humile* under current climatic scenarios in China.

3.4. The Changes Potential Suitable Areas of Linepithema humile under Future Climatic Scenarios

The potential suitable areas of *L. humile* under the SSP1-2.6, SSP2-4.5, and SSP5-8.5 scenarios, in the 2030s and 2050s are shown in Figures 7 and 8. The potential suitable areas were mainly located in Jiangsu, Zhejiang, Fujian, Jiangxi, Anhui, Hunan, Hubei, and Yunnan. The results showed that the potential suitable areas increased under the future climatic scenarios. The loss areas were mainly located in Fujian, Jiangxi, Guangxi, Yunnan, and Anhui. The gain areas were mainly located in Jiangsu, Anhui, Hubei, Sichuan, and Henan.

Under the SSP1-2.6 scenario in 2030s, the total, highly, moderately, and poorly suitable areas of *L. humile* were 104.60 × 10^4 km^2, 0.54 × 10^4 km^2, 9.22 × 10^4 km^2, and 94.84 × 10^4 km^2 (Table S2), respectively, accounting for 10.90%, 0.06%, 0.96%, and 9.88% of the area of Chinese mainland, respectively. Under the SSP1-2.6 scenario in 2050s, the total, highly, moderately, and poorly suitable areas of *L. humile* were 116.10 × 10^4 km^2, 0.76 × 10^4 km^2, 13.43 × 10^4 km^2, and 101.91 × 10^4 km^2, respectively, accounting for 12.09%, 0.08%, 1.40%, and 10.61% of the area of Chinese mainland, respectively. In the 2030s and 2050s, under

SSP1-2.6, the total, highly, moderately, and poorly suitable areas gradually increased (Figure 7).

Under the SSP1-2.6 scenario in 2030s and 2050s, the loss areas were 9.24×10^4 km^2, and 7.59×10^4 km^2 (Table S3), respectively, which was mainly located in Anhui, Jiangxi, Fujian, Guangxi, Chongqing, and Sichuan. The gain areas were 33.21×10^4 km^2, and 43.10 $\times 10^4$ km^2, respectively, which were mainly located in Anhui, Jiangsu, Hubei, Sichuan, Henan, and Guangdong (Figure 8).

Under the SSP2-4.5 scenario in 2030s, the total, highly, moderately, and poorly suitable areas of *L. humile* were 102.50×10^4 km^2, 0.59×10^4 km^2, 11.07×10^4 km^2, and 90.84×10^4 km^2, respectively, accounting for 10.67%, 0.06%, 1.15%, and 9.46% of the area of the Chinese mainland, respectively. Under the SSP2-4.5 scenario in 2050s, the total, highly, moderately, and poorly suitable areas of *L. humile* were 95.03×10^4 km^2, 0.49×10^4 km^2, 15.73×10^4 km^2, and 78.81×10^4 km^2, respectively, accounting for 9.90%, 0.05%, 1.64%, and 8.21% of the area of Chinese mainland, respectively. In the 2030s and 2050s, under SSP2-4.5, the total, highly, moderately, and poorly suitable areas gradually increased.

Under the SSP2-4.5 scenario in 2030s and 2050s, the loss areas were 9.45×10^4 km^2, and 16.56×10^4 km^2, respectively, which were mainly located in Anhui, Chongqing, Yunnan, Guangxi, Guangdong, and Sichuan. The gain areas were 31.56×10^4 km^2, and 31.23×10^4 km^2, respectively, which were mainly located in Anhui, Jiangsu, Hubei, Sichuan, Henan, and Guizhou.

Under the SSP5-8.5 scenario in 2030s, the total, highly, moderately, and poorly suitable areas of *L. humile* were 97.69×10^4 km^2, 0.87×10^4 km^2, 7.22×10^4 km^2, and 89.60×10^4 km^2, respectively, accounting for 10.17%, 0.09%, 0.75%, and 9.33% of the area of Chinese mainland, respectively. Under the SSP5-8.5 scenario in 2050s, the total, highly, moderately, and poorly suitable areas of *L. humile* were 73.04×10^4 km^2, 1.12×10^4 km^2, 4.26×10^4 km^2, and 67.66×10^4 km^2, respectively, accounting for 7.61%, 0.12%, 0.44%, and 7.05% of the area of Chinese mainland, respectively. In the 2030s and 2050s, under SSP5-8.5, the total, moderately, and poorly suitable areas gradually decreased, while the highly suitable area increased.

Under the SSP5-8.5 scenario in 2030s and 2050s, the loss areas were 11.78×10^4 km^2, and 26.11×10^4 km^2, respectively, which were mainly located in Anhui, Jiangxi, Yunnan, Chongqing, Fujian, and Guangxi. The gain areas were 28.91×10^4 km^2, and 18.92×10^4 km^2, respectively, which were mainly located in Anhui, Jiangsu, Hubei, Sichuan, and Henan.

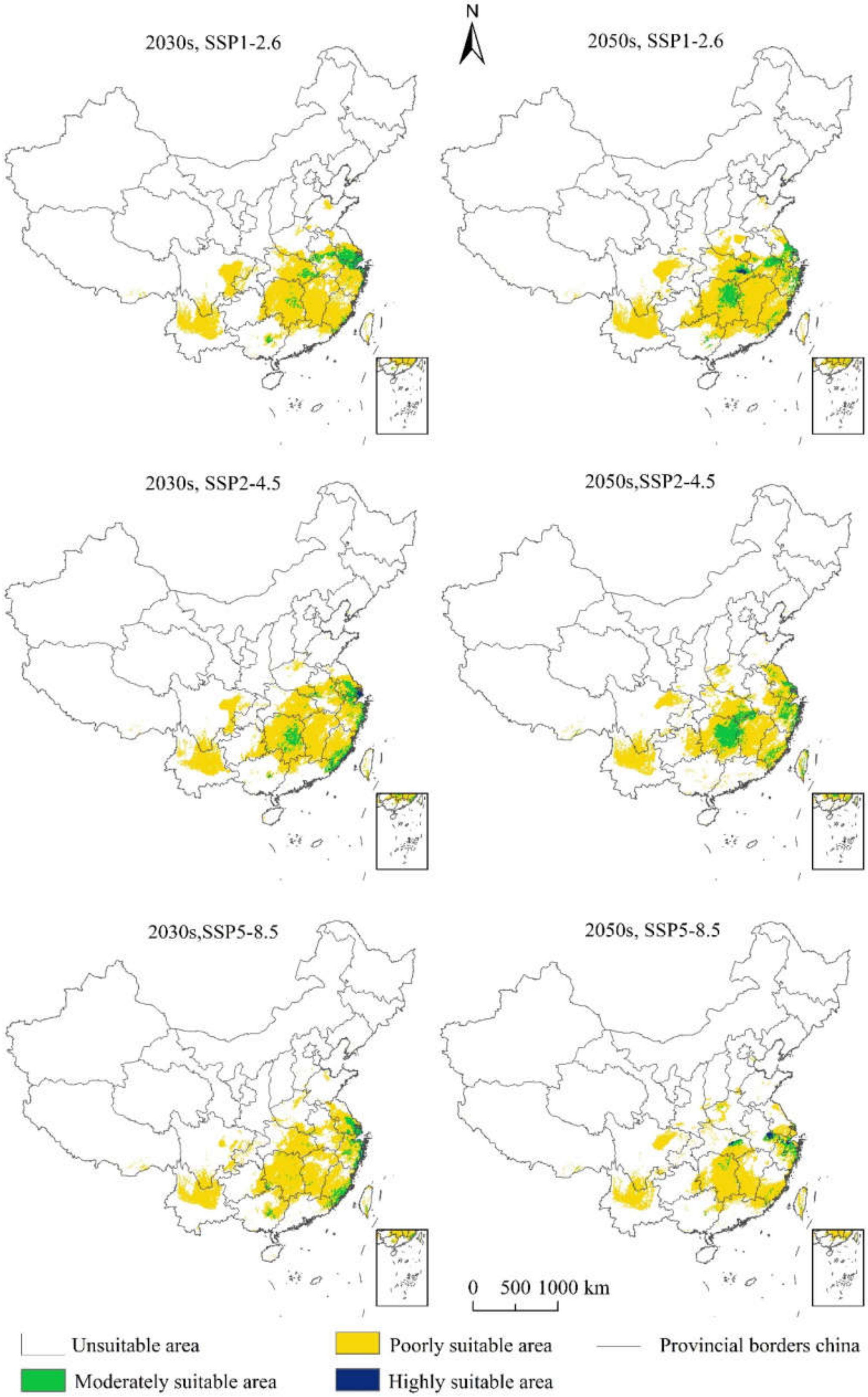

Figure 7. Potential suitable area for *Linepithema humile* under future climate scenarios in China.

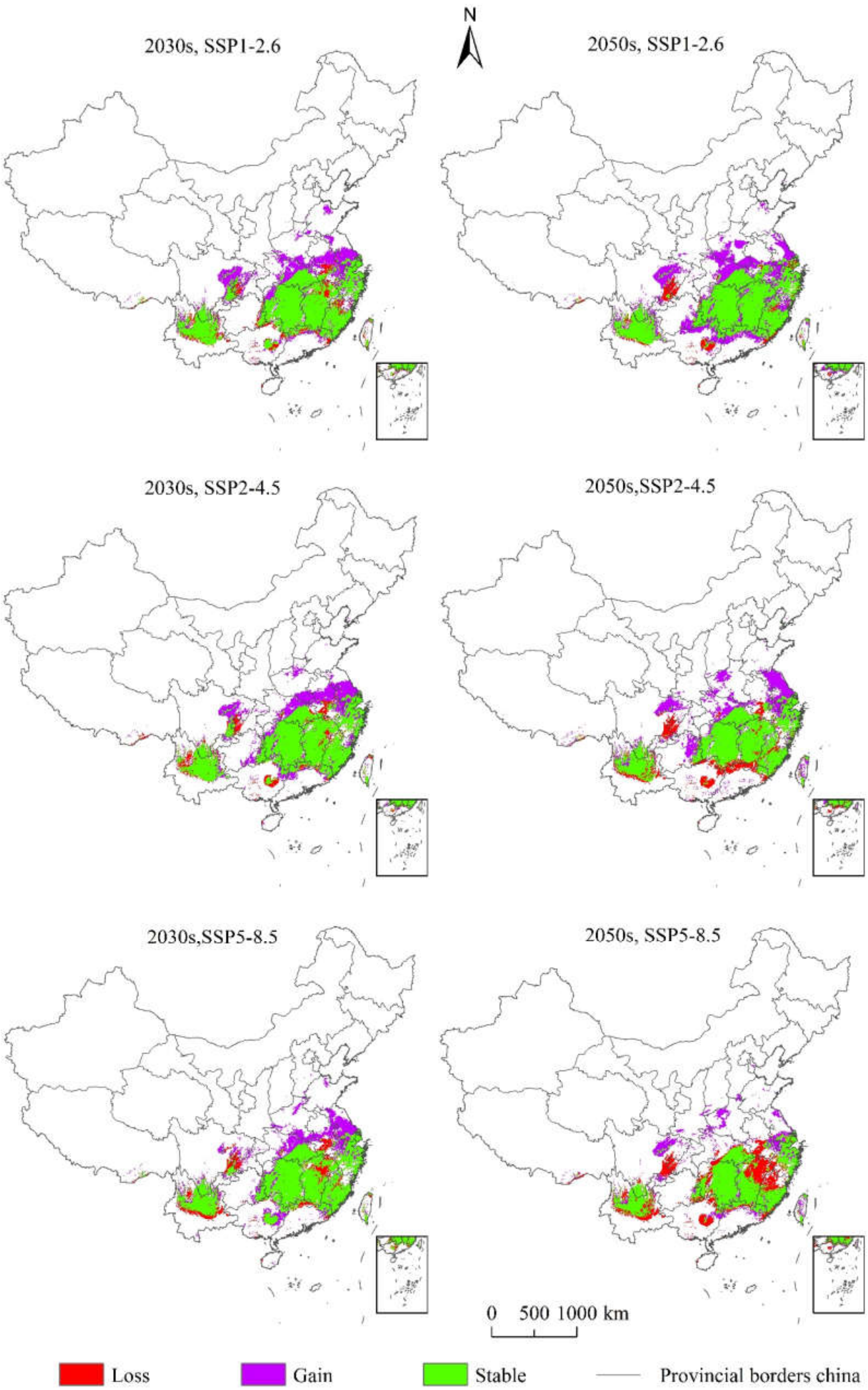

Figure 8. Changes in potential suitable areas for *Linepithema humile* between the current and future climatic scenarios in China.

3.5. The Centroid Migration of Potential Suitable Areas for Linepithema humile

The centroids of potential suitable areas of *L. humile* in China under current and future climate scenarios are shown in Figure 9. The centroid of potential suitable areas of *L. humile* shifted to northward and high-latitude areas under future climate scenarios.

Under the current climate, the centroid of the potential suitable area was located at the point (112.38° E, 27.28° N). Under SSP1-2.6 scenario, the suitable areas of 2030s and 2050s centroids were to the point (112.70° E, 28.33° N) and the point (112.59° E, 28.11° N), it shifted 0.32° E and 1.05° N from the current to the 2030s, 0.11° E and 0.22° N from the 2030s to the 2050s. Under SSP2-4.5 scenario, the suitable areas of 2030s and 2050s centroids were to the point (112.96° E, 28.13° N) and the point (112.94° E, 28.53° N), it shifted 0.58° E and 0.85° N from the current to the 2030s, 0.02° E and 0.40° N from the 2030s to the 2050s. Under SSP5-8.5 scenario, the suitable areas of 2030s and 2050s centroids were to the point (112.92° E, 28.19° N) and the point (112.54° E, 27.96° N), it shifted 0.54° E and 0.91° N from the current to the 2030s, 0.38° E and 0.23° N from the 2030s to the 2050s.

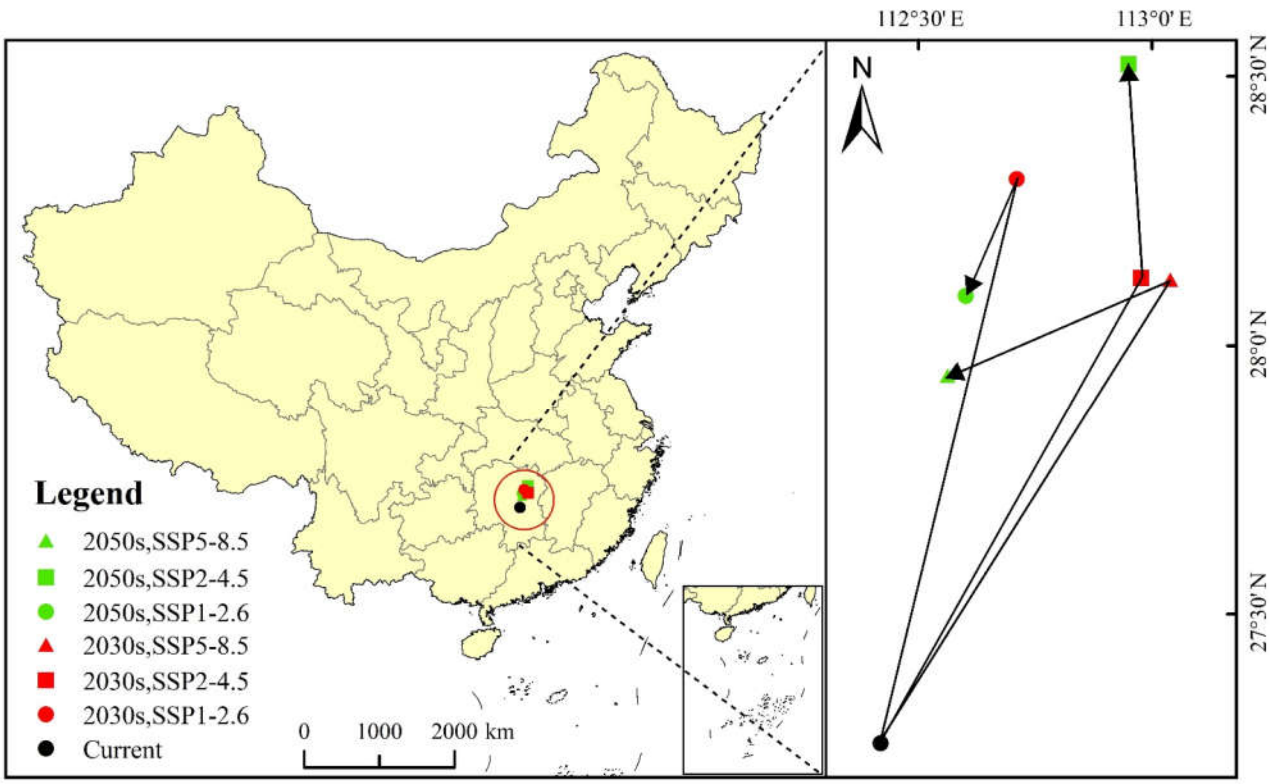

Figure 9. Distribution centroids of *Linepithema humile* under current and future climatic scenarios in China.

4. Discussion

The important bioclimatic variables affecting the potential suitable areas of *L. humile* in China were mean temperature of the coldest quarter (Bio11) and mean temperature of the wettest quarter (Bio8), precipitation of the coldest quarter (Bio19), and precipitation of the warmest quarter (Bio18). Our results showed that the presence probability of *L. humile* gradually increased when the mean temperature of the coldest quarter (Bio11) was −3.42–11.45 °C, and gradually decreased when it was 11.45–27.79 °C. The probability of *L. humile* was less change when the mean temperature of the wettest quarter (Bio8) was 6.63–18.34 °C, gradually increased when it was 18.41–27.88 °C, and gradually decreased when it was 27.88–29.91 °C. This would suggest that they prefer warm, wet climates over cold, wet conditions. This is consistent with previous studies. Temperature within a range from 18 to 32 °C has been established to influence all stages of *L. humile* development from eggs to adults, with development time being shortened at higher temperatures [38]. *Linepithema humile* stops feeding when the temperature is consistently below 5 °C, and the colony eventually starves to death [39]. The oviposition rate of *L. humile* was affected at laboratory temperatures ranging between 10 and 34 °C, and under different polygamous conditions, which oviposition highest at 28 °C [40].

Precipitation variables also had direct and indirect effects on the distribution patterns of *L. humile*. Changes in precipitation affect the humidity and temperature of *L. humile* habitats, and thereby affect growth and development, survival, reproduction, and overwintering [41–43]. Our results indicate that the probability of the presence of *L. humile* was greatly affected by the precipitation of the coldest quarter. Previous study showed that elevated soil moisture increased the populations of *L. humile*, and their ability to compete with native ant species [44]. Cessation of irrigation resulted in a population decline of *L. humile* in San Diego, USA [44].

The prediction of potential suitable areas of IAS is an important element for invasion risk assessment, identifying the potential suitable areas of *L. humile* in China can provide scientific guidance for the early monitoring, prevention, and control of *L. humile*. Our results showed that the potential suitable areas for *L. humile* under the current climate were mainly located in eastern, central and southwestern China. Under future climate scenario, the potential suitable areas generally showed an increasing trend. The mild climate and abundant moisture in the coastal areas of southeastern China provide suitable conditions for the invasion of *L. humile* [45]. Previous studies have indicated that climate warming increases the distribution areas of IAS. For instance, the global distribution areas of Zeuzera pyrina and Ceroplastes cirripediformis will increase under future climate scenarios and will expand to temperate regions worldwide [46,47]. The prediction of distribution areas of the 13 most invasive termites worldwide, indicated that the distribution areas of 12 species would likely increase under future climate scenarios [48]. There is some consistency between the results of the above studies and the those of this study.

As global climate continues to warm, many insects have shifted to high-latitude areas [49]. Our results showed that the centroid of potential suitable area of *L. humile* in China shifted to high-latitude areas under future climate scenarios. Previous studies showed that the potential suitable areas of *S. invicta* and *Hyphantria cunea* in China also shifted to high-latitude areas under all future climate scenarios [50,51]. These studies also verified our results and the hypothesis that insects will move to high-latitude areas with increasing global warming [52,53].

The global dispersal pathways of *L. humile* are mainly natural dispersal, global trade, and accidental dispersal [54,55]. The maximum possible invasion in China would be due to accidental dispersal. There are many vectors for accidental spread, including containers and packaging-wood, human-related waste, sod and mulch, plants or parts of plants, soil, and gravel [56]. When *L. humile* was introduced into a new habitat, they spread rapidly by natural dispersal and vectorial transport. Eastern, central and southwestern coastal areas of China were the potential suitable areas of *L. humile*, which is also the area at the highest risk of invasion, due to the large number of ports receiving international cargo. Zhejiang, Fujian, Jiangxi, Anhui, Hunan, Hubei, Yunnan, and Sichaun areas of China were the potential suitable areas of *L. humile*, which is also the area at the highest risk of invasion, due to the large number of ports receiving international cargo. Therefore, Hangzhou, Fuzhou, Nanchang, Hefei, Changsha, Wuhan, Kunming, and Chengdu customs should strengthen the quarantine of the logs, wooden packaging, and containers that was from Europe and America. If a wild population of *L. humile* is found in China, it should immediately be eradicated using cultural, biological and chemical control measures [56]. Cultural control measures mainly involve applying powder barriers and limiting access to water sources or nesting sites [44]. Biological control measures are more difficult, because of the lack of natural enemies of the species [57]. Chemical control measures are more widely used to prevent *L. humile* from entering an area, such as barrier treatment with contact-residual insecticides and baits, but these only kill actively feeding ants and barely affect the larvae or queen [58]. Finally, a comprehensive risk assessment system for the early warning, quarantine, and control of *L. humile* invasion was established.

5. Conclusions

We are the first to use an optimized MaxEnt models to explore the distribution pattern and limiting bioclimatic variables of *L. humile* in China. The high invasion risk areas were mainly located in Zhejiang, Fujian, Jiangxi, Anhui, Hunan, Hubei, Yunnan, and Sichaun. Moreover, the risk of invasion of *L. humile* in China will further increase under future climate scenarios. The mean temperature of the coldest quarter was the most significant bioclimatic variable affecting the distribution pattern of *L. humile* in China. Our study highlights the importance of climate change on the invasion of *L. humile* and could help formulate targeted early warning, prevention and control policies for *L. humile* in China.

Supplementary Materials: The following supporting information can be downloaded at: www.mdpi.com/1424-2818/14/11/921/s1, Figure S1: Correlation coefficient between Bioclimatic variables; Figure S2: Contribution of different bioclimatic variables to MaxEnt model for *Linepithema humile*; Table S1: Three emission scenarios; Table S2: Potential suitable areas for *Linepithema humile* under different climate change scenarios (10^4 km^2); Table S3: Future changes in suitable area ($10^4 km^2$).

Author Contributions: M.L., X.X. and W.L.: conception and design of the research. M.L. and X.X.: acquisition of data. M.L., X.X. and H.Z.: analysis and interpretation of data. M.L. and X.X.: statistical analysis. M.L., X.X. and H.Z.: drafting the manuscript. L.X., H.H., B.C., W.L., and F.W.: manuscript revision. All authors have read and agreed to the published version of the manuscript.

Funding: This project was funded by the National Key R&D Program of China (grant no. 2021YFC2600400), the Science and Technology Innovation Program of Chinese Academy of Agricultural Sciences (grant no. caascx-2017-2022-IAS).

Institutional Review Board Statement: Not applicable.

Data Availability Statement: The data presented in this study are available in this article.

Conflicts of Interest: The authors declare that the research was conducted in the absence of any commercial or financial relationships that could be construed as a potential conflict of interest.

References

1. Cheng, B.X.; Sun, Y.F.; Han, Z.H.; Huang, H.K.; Zhang, H.B.; Li, Y.K.; Zhang, G.L.; Liu, W.X. Challenges in preventing and controlling invasive alien species in China. *J. Biosaf.* **2020**, *29*, 157–163.
2. Capinha, C.; Essl, F.; Seebens, H.; Moser, D.; Pereira, H.M. The dispersal of alien species redefines biogeography in the Anthropocene. *Science* **2015**, *348*, 1248–1251.
3. Seebens, H.; Essl, F.; Blasius, B. The intermediate distance hypothesis of biological invasions. *Ecol. Lett*. **2017**, *20*, 158–165.
4. Li, H.R.; Yan, J.; Du, C.; Yan, X.L. Current status and suggestions of research on invasive risk assessment of alien plants in China. *Acta Ecol. Sin*. **2022**, *42*, 6451–6463.
5. Wu, J.Q.; Smith, M.T. Successful Approaches for Battling Invasive Species in Developed Countries. *Acta Agric. Univ. Jiangxiensis* **2010**, *32*, 1040–1055.
6. Angulo, E.; Hoffmann, B.D.; Ballesteros-Mejia, L.; Taheri, A.; Balzani, P.; Bang, A.; Renault, D.; Cordonnier, M.; Bellard, C.; Diagne, C.; et al. Economic costs of invasive alien ants worldwide. *Biol. Invasions.* **2022**, *24*, 2041–2060.
7. Luque, G.M.; Bellard, C.; Cleo, B.; Bonnaud, E.; Genovesi, P.; Simberloff, D.; Courchamp, F. The 100th of the world's worst invasive alien species. *Biol. Invasions*. **2014**, *16*, 981–985.
8. Mothapo, N.P.; Wossler, T.C. Behavioural and chemical evidence for multiple colonisation of the Argentine ant, *Linepithema humile*, in the Western Cape, South Africa. *BMC Ecol*. **2011**, *11*, 1–11.
9. Ingram, K.K. Plasticity in Queen Number and Social Structure in The Invasive Argentine Ant (*Linepithema Humile*). *Evolution* **2002**, *56*, 2008–2016.
10. Kennedy, T.A. Patterns of an invasion by Argentine ants (*Linepithema humile*) in a riparian corridor and its effects on ant diversity. *Am. Midl. Nat.* **1998**, *140*, 343–350.

11. Lach, L. A mutualism with a native membracid facilitates pollinator displacement by Argentine ants. *Ecology* **2007**, *88*, 1994–2004.
12. Lach, L. Argentine ants displace floral arthropods in a biodiversity hotspot. *Divers. Distrib*. **2008**, *14*, 281–290.
13. Ward, D.F.; Green, C.; Harris, R.J.; Hartley, S.; Lester, P.J.; Stanley, M.C.; Suckling, D.M.; Toft, R.J. Twenty years of Argentine ants in New Zealand: Past research and future priorities for applied management. *N. Z. Entomol*. **2010**, *33*, 68–78.
14. Zhao, H.X.; Xian, X.Q.; Zhao, Z.H.; Zhang, G.F.; Liu, W.X.; Wan, F.H. Climate Change Increases the Expansion Risk of *Helicoverpa zea* in China According to Potential Geographical Distribution Estimation. *Insects* **2022**, *13*, 79.
15. Newman, J.A. Climate change and the fate of cereal aphids in Southern Britain. *Glob. Change Biol*. **2005**, *11*, 940–944.
16. Menzel, F.; Feldmeyer, B. How does climate change affect social insects? *Curr. Opin. Insect. Sci*. **2021**, *46*, 10–15.
17. Zhao, G.H.; Cui, X.Y.; Sun, J.J.; Li, T.T.; Wang, Q.; Ye, X.Z.; Fan, B.G. Analysis of the distribution pattern of Chinese Ziziphus jujuba under climate change based on optimized biomod2 and MaxEnt models. *Ecol. Indic*. **2021**, *132*, 108256.
18. Wang, H.R.; Zhang, Q.Z.; Liu, R.F.; Sun, Y.; Xiao, J.H.; Gao, L.; Gao, X.; Wang, H.B. Impacts of changing climate on the distribution of *Solenopsis invicta* Buren in Mainland China: Exposed urban population distribution and suitable habitat change. *Ecol. Indic*. **2022**, *139*, 108944.
19. Elith, J.; Leathwick, J.R. Species distribution models: Ecological explanation and prediction across space and time. *Ann. Rev. Ecol. Evol. System*. **2009**, *40*, 677–697.
20. Guisan, A.; Thuiller, W.; Zimmermann, N.E. *Habitat Suitability and Distribution Models: With Applications in R*; Cambridge University Press: Cambridge, UK, 2017.
21. Zhang, X.Q.; Li, G.Q.; Du, S. Simulating the potential distribution of *Elaeagnus angustifolia* L. based on climatic constraints in China. *Ecol. Eng*. **2018**, *113*, 27–34.
22. Phillips, S.J.; Anderson, R.P.; Schapire, R.E. Maximum entropy modeling of species geographic distributions. *Ecol. Modell*. **2006**, *190*, 231–259.
23. Zhang, K.L.; Yao, L.J.; Meng, J.S.; Tao, J. Maxent modeling for predicting the potential geographical distribution of two peony species under climate change. *Sci. Total Environ*. **2018**, *634*, 1326–1334.
24. Li, J.J.; Fan, G.; He, Y. Predicting the current and future distribution of three Coptis herbs in China under climate change conditions, using the MaxEnt model and chemical analysis. *Sci. Total Environ*. **2020**, *698*, 134141.
25. Zhang, X.A.; Sui, X.Y.; Lv, Z.; Chen, Y.F. A prediction of the global habitat of two invasive fishes (*Pseudorasbora parva* and *Carassius auratus*) from East Asia using MaxEnt. *Biodivers. Sci*. **2014**, *22*, 182–188.
26. Zhang, H.; Song, J.Y.; Zhao, H.X.; Li, M.; Han, W.H. Predicting the distribution of the invasive species *Leptocybe invasa*: Combining MaxEnt and Geodetector models. *Insects* **2021**, *12*, 92.
27. Liu, X.Y.; Zhao, C.Y.; Li, F.F.; Zhu, J.F.; Gao, K.X.; Hu, Y.B. Prediction of potential geographical distribution of *Solenopsis invicta* Buren in China based on MaxEnt. *Plant Quar.* **2019**, *33*, 70–76.
28. Zhang, Y.J.; Ma, F.Z.; Xu, H.G.; Fan, J.Y.; Sun, H.Y.; Ding, H. Prediction of potential geographic distribution of *Anoplolepis gracilipes* (Homoptera: Formicinae) in China using MaxEnt model. *Chin. J. Ecol.* **2018**, *37*, 3364–3370.
29. Warren, D.L.; Seifert, S.N. Ecological niche modeling in Maxent: The importance of model complexity and the performance of model selection criteria. *Ecol. Appl*. **2011**, *21*, 335–342.
30. Warren, D.L.; Wright, A.N.; Seifert, S.N.; Shaffer, H.B. Incorporating model complexity and spatial sampling bias into ecological niche models of climate change risks faced by 90 California vertebrate species of concern. *Divers. Distrib*. **2014**, *20*, 334–343.
31. Zhu, G.P.; Qiao, H.J. Effect of the Maxent model's complexity on the prediction of species potential distributions. *Biodivers. Sci*. **2016**, *24*, 1189–1196.
32. Bowen, A.K.M.; Stevens, M.H.H. Temperature, topography, soil characteristics, and NDVI drive habitat preferences of a shade-tolerant invasive grass. *Ecol. Evol*. **2020**, *10*, 10785–10797.
33. Merow, C.; Smith, M.J.; Silander, J.A., Jr. A practical guide to MaxEnt for modeling species' distributions: What it does, and why inputs and settings matter. *Ecography* **2013**, *36*, 1058–1069.
34. Zhu, G.P.; Liu, Q.; Gao, Y.B. Improving ecological niche model transferability to predict the potential distribution of invasive exotic species. *Biodivers. Sci*. **2014**, *22*, 223–230.
35. Moreno, R.; Zamora, R.; Molina, J.R.; Vasquez, A.; Herrera, M.Á. Predictive modeling of microhabitats for endemic birds in South Chilean temperate forests using Maximum entropy (Maxent). *Ecol. Inform*. **2011**, *6*, 364–370.
36. Swets, J.A. Measuring the accuracy of diagnostic systems. *Science* **1988**, *240*, 1285–1293.
37. Zhang, M.Z.; Ye, X.Z.; Li, J.H.; Liu, Y.P.; Chen, S.P.; Liu, B. Prediction of potential suitable area of Ulmus elongate in China under climate change scenarios. *Chin. J. Ecol*. **2021**, *40*, 3822–3835.
38. Abril, S.; Oliveras, J.; Gómez, C. Effect of temperature on the development and survival of the Argentine ant, *Linepithema humile*. *J. Insect Sci*. **2010**, *10*, 97.
39. Brightwell, R.J.; Labadie, P.E.; Silverman, J. Northward expansion of the invasive *Linepithema humile* (Hymenoptera: Formicidae) in the Eastern United States is constrained by winter soil temperatures. *Environ. Entomol*. **2010**, *39*, 1659–1665.
40. Abril, S.; Oliveras, J.; Gómez, C. Effect of temperature on the oviposition rate of Argentine ant queens (*Linepithema humile* Mayr) under monogynous and polygynous experimental conditions. *J. Insect Physiol*. **2007**, *54*, 265–272.
41. Battisti, A.; Stastny, M.; Netherer, S.; Robinet, C.; Schopf, A.; Roques, A.; Larsson, S. Expansion of geographic range in the pine processionary moth caused by increased winter temperatures. *Ecol. Appl*. **2005**, *15*, 2084–2096.

42. Zhu, H.; Wang, D.L.; Wang, L.; Fan, J.; Sun, W.; Ren, B.Z. Effects of altered precipitation on insect community composition and structure in a meadow steppe. *Ecol. Entomol*. **2014**, *39*, 453–461.
43. Chang, X.N.; Gao, X.N.; Cheng, F.J.; Zhai, B.P. Effects of environmental moisture and precipitation on insects: A review. *Chin. J. Ecol*. **2008**, *27*, 619–625.
44. Menke, S.B.; Holway, D.A. Abiotic factors control invasion by Argentine ants at the community scale. *J. Animal Ecol*. **2006**, *75*, 368–376.
45. Vega, S.J.; Rust, M.K. The Argentine ant–a significant invasive species in agricultural, urban and natural environment. *Sociobiology* **2001**, *37*, 3–25.
46. Wang, F.; Wang, D.; Guo, G.; Zhang, M.X.; Lang, J.Y.; Wei, J.F. Potential distributions of the invasive barnacle scale *Ceroplastes cirripediformis* (Hemiptera: Coccidae) under climate change and implications for its management. *J. Econ. Entomol*. **2020**, *114*, 82–89.
47. Fekrat, L.; Farashi, A. Impacts of climatic changes on the worldwide potential geographical dispersal range of the leopard moth, *Zeuzera pyrina* (L.) (Lepidoptera: Cossidae). *Glob. Ecol. Conserv*. **2022**, *34*, e02050.
48. Buczkowski, G.; Bertelsmerier, C. Invasive termites in a changing climate: A global perspective. *Ecol. Evol*. **2017**, *7*, 974–985.
49. Li, X.; Ge, X.Z.; Chen, L.H.; Zhang, L.J.; Wang, T.; Zong, S.X. Climate change impacts on the potential distribution of *Eogystia hippophaecolus* in China. *Pest. Manag. Sci*. **2018**, *75*, 215–223.
50. Song, J.Y.; Zhang, H.; Li, M.; Han, W.H.; Yin, Y.X.; Lei, J.P. Prediction of spatiotemporal invasive risk of the red import fire ant, *Solenopsis invicta* (Hymenoptera: Formicidae), in China. *Insects* **2021**, *12*, 874.
51. Ji, Y.L.; Su, X.Y.; Yu, Z.J. Potential habitat prediction of *Hyphantria cunea* based on random forest model in China. *J. Nanjing Univ. Nat. Sci*. **2019**, *43*, 121–128.
52. Zhang, V.M.; Punzalan, D.; Rowe, L. Climate change has different predicted effects on the range shifts of two hybridizing ambush bug (*Phymata, Family Reduviidae*, Order Hemiptera) species. *Ecol. Evol*. **2020**, *10*, 12036–12048.
53. Chapman, J.W.; Bell, J.R.; Burgin, L.E.; Reynolds, D.R.; Pettersson, L.B.; Hill, J.K.; Bonsall, M.B.; Thomas, J.A. Seasonal migration to high latitudes results in major reproductive benefits in an insect. *Proc. Natl. Acad. Sci. USA* **2012**, *109*, 14924–14929.
54. Carpintero, S.; Reyes-López, J.; Reyna, L.A.D. Impact of Argentine ants (*Linepithema humile*) on an arboreal ant community in Doñana National Park, Spain. *Biodivers. Conserv*. **2005**, *14*, 151–163.
55. Suarez, A.V.; Holway, D.A.; Case, T.J. Patterns of spread in biological invasions dominated by long-distance jump dispersal: Insights from Argentine ants. *Proc. Natl. Acad. Sci. USA* **2001**, *98*, 1095–1100.
56. CABI. *Invasive Species Compendium of the Center for Agriculture and Bioscience International*; Wallingford, UK: CAB International 2022. Available online: https://www.cabi.org/isc (accessed on 28 June 2022).
57. Orr, M.R.; Seike, S.H.; Benson, W.W.; Dahlsten, D.L. Host specificity of *Pseudacteon* (Diptera: Phoridae) parasitoids that attack *Linepithema* (Hymenoptera: Formicidae) in South America. *Environ. Entomol*. **2001**, *30*, 742–747.
58. Rust, M.K. Insecticides and their use in urban structural pest control. In *Handbook of Pesticide Toxicology*, 2nd ed.; Academic Press San Diego USA, 2001; pp. 243–250.